

TABLE I. Excitation ( $\gamma_{12}$ , left column) and de-excitation ( $\gamma_{21}$ , right column) rates for NPIs between the ground state and first excited state of a  $^{188}\text{Os}$  nucleus for different temperatures and densities, calculated using the ISOMEX code [25].

Density	$\mathcal{T} = 0.01$ MeV	$\mathcal{T} = 0.1$ MeV	$\mathcal{T} = 1$ MeV
$10 \text{ g/cm}^3$	$6.0 \cdot 10^2 / 6.5 \cdot 10^8 \text{ s}^{-1}$	$7.3 \cdot 10^8 / 6.9 \cdot 10^8 \text{ s}^{-1}$	$1.6 \cdot 10^{10} / 3.8 \cdot 10^9 \text{ s}^{-1}$
$10^3 \text{ g/cm}^3$	$7.0 \cdot 10^2 / 7.6 \cdot 10^8 \text{ s}^{-1}$	$7.3 \cdot 10^8 / 6.9 \cdot 10^8 \text{ s}^{-1}$	$1.6 \cdot 10^{10} / 3.8 \cdot 10^9 \text{ s}^{-1}$
$10^5 \text{ g/cm}^3$	$8.0 \cdot 10^2 / 8.6 \cdot 10^8 \text{ s}^{-1}$	$7.8 \cdot 10^8 / 7.3 \cdot 10^8 \text{ s}^{-1}$	$1.6 \cdot 10^{10} / 3.8 \cdot 10^9 \text{ s}^{-1}$

check that the results converge [18]. This serves as verification of the method and a baseline that allows us to evaluate the thermal effects of the plasma.

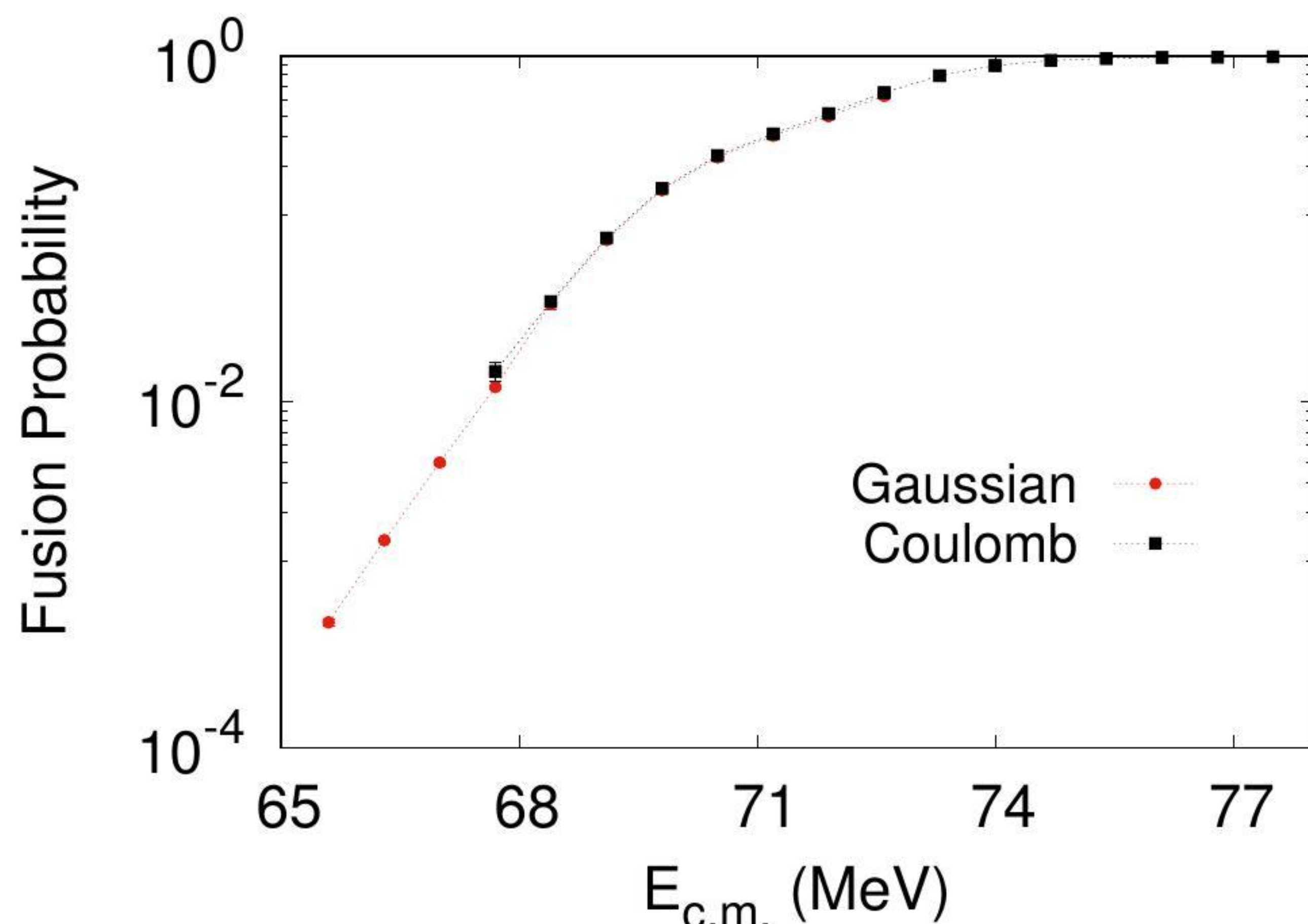


FIG. 1. A construction of the energy-resolved fusion probability for a  $^{16}\text{O}$  projectile and  $^{188}\text{Os}$  target with coupled channels but without a plasma environment ( $\mathcal{T} = 0$  MeV). Gaussian and Coulomb wave packets are used, taking the average energy-resolved fusion probability for a range of incident mean energies,  $E_0$ . Error bars due to statistical error are included but most are insignificant. The nominal Coulomb barrier between these nuclei is 71.7 MeV.

Fig. 2 shows the population of the radial grid basis states over time for an initial Gaussian wave packet with an average energy  $E_0 = 70$  MeV and a temperature  $\mathcal{T} = 0.1$  MeV. The change of population of both the ground state (elastic channel) and the  $2^+$  excited state of  $^{188}\text{Os}$  (inelastic channel) due to both thermal effects and the radial coupling between these states can be observed.

To isolate the effects of temperature on fusion probability, the increase in energy-resolved fusion probability was calculated using the ratio between coupled channels calculations at either  $\mathcal{T} = 0.1$  MeV or  $\mathcal{T} = 0.5$  MeV and  $\mathcal{T} = 0$  MeV, shown in Fig. 3. The fusion probability was calculated by taking the average energy-resolved fusion probability for initial wave packets with varying  $E_0$ . For  $\mathcal{T} = 0.1$  MeV, the green (square) points were calculated using a Gaussian wave packet with  $E_0 = 60, 63, 65, 67$  and  $70$  MeV, and the blue (circle) points were calculated using a Coulomb wave packet with  $E_0 = 65, 67$  and  $70$  MeV. The same method was used for both

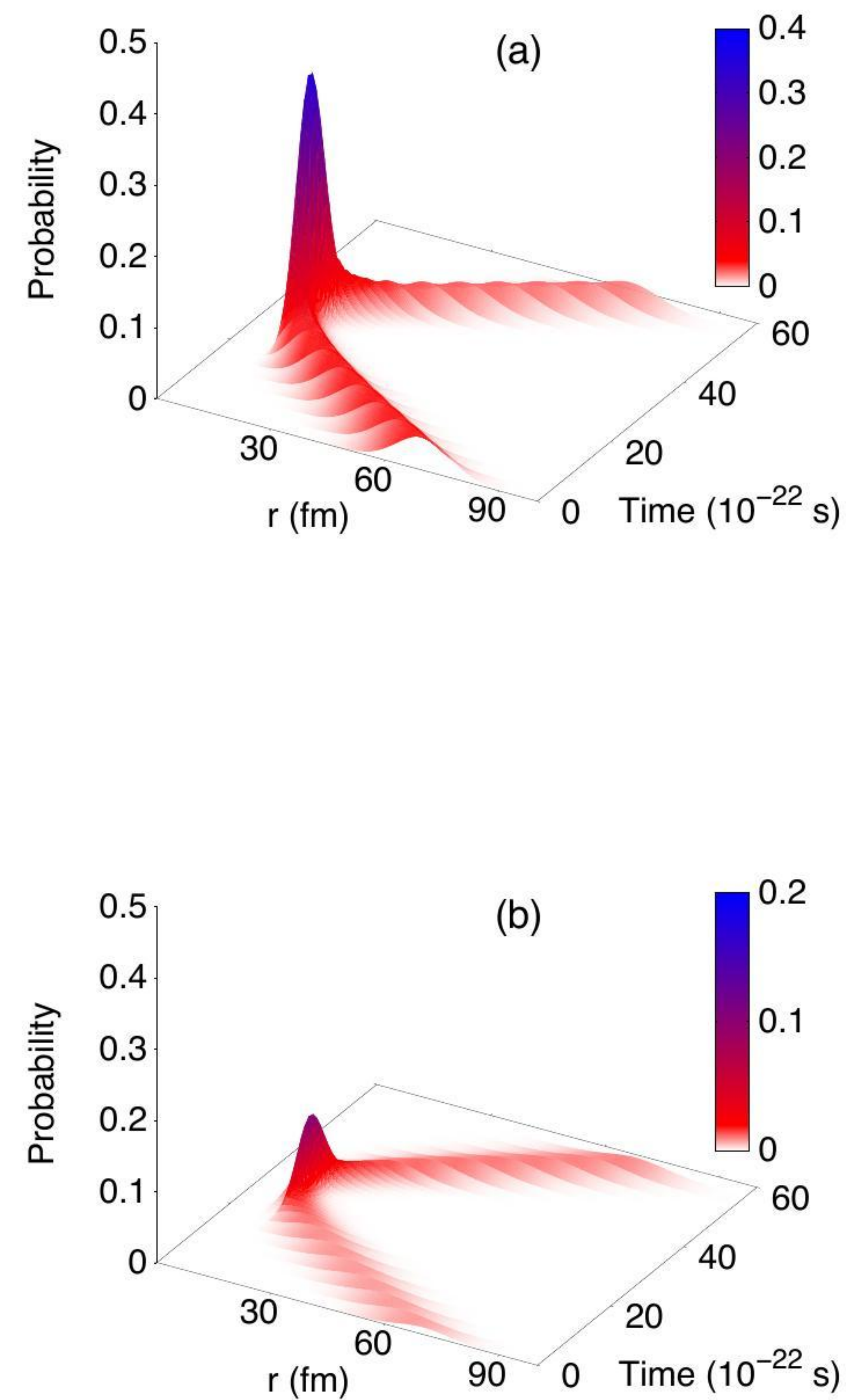


FIG. 2. Radial position probability as a function of internuclear radius and time for a head-on collision of  $^{16}\text{O} + ^{188}\text{Os}$  with  $E_0 = 70$  MeV and  $\mathcal{T} = 0.1$  MeV. The radial probability changes for (a) the elastic and (b) inelastic channels respectively, as the nuclei approach their Coulomb barrier ( $r \approx 11.5$  fm). The inelastic channel is thermally populated before the target and projectile interact with each other. For visualisation, when the mean radius is larger than 20 fm, the time step is  $3 \times 10^{-22}$  s.

$\mathcal{T} = 0$  and  $\mathcal{T} = 0.5$  MeV. The error bars associated with these points are simply due to the standard error in the mean. We use a Gaussian wave packet for its accuracy at deep sub-barrier energies compared to a Coulomb wave packet. However, a Coulomb wave packet offers a better global description of fusion probability around and above